Science Advances
AAAS

advances.sciencemag.org/cgi/content/full/6/40/eabc4149/DC1

Supplementary Materials for

Ancient and conserved functional interplay between Bcl-2 family proteins in the mitochondrial pathway of apoptosis

Nikolay Popgeorgiev*, Jaison D Sa, Lea Jabbour, Suresh Banjara, Trang Thi Minh Nguyen, Aida Akhavan-E-Sabet, Rudy Gadet, Nikola Ralchev, Stéphen Manon, Mark G. Hinds, Hans-Jürgen Osigus, Bernd Schierwater, Patrick O. Humbert, Ruth Rimokh, Germain Gillet*, Marc Kvansakul*

*Corresponding author. Email: nikolay.popgeorgiev@univ-lyon1.fr (N.P.); germain.gillet@univ-lyon1.fr (G.G.); m.kvansakul@latrobe.edu.au (M.K.)

Published 30 September 2020, *Sci. Adv.* **6**, eabc4149 (2020)
DOI: 10.1126/sciadv.abc4149

This PDF file includes:

Supplementary Materials

Supplementary Table S1: X-ray crystallographic data collection and refinement statistics

	trBcl-2L2:trBak BH3	hsBcl-x_L:trBak BH3
Data collection		
Space group	P1	$P2_1$
Cell dimensions a, b, c (Å) α, β, γ (°)	 34.30, 40.86, 56.72 97.3 90.09 101.09	 39.20, 63.86, 69.87 90.00 94.58 90.00
Wavelength (Å)	0.9537	0.9537
Resolution (Å)	39.83-1.40 (1.40-1.42)	37.07-1.90 (1.90-1.95)
R_{sym} or R_{merge}	0.076 (1.16)	0.125 (1.74)
I / σI	6.7 (0.6)	6.4 (0.7)
Completeness (%) $CC_{1/2}$	95.1 (84.0) 0.99 (0.358)	98.2 (97.5) 0.99 (0.351)
Redundancy	3.6 (3.5)	5.5 (5.6)
Refinement		
No. reflections	56404	26735
R_{work} / R_{free}	0.186/213	0.199/236
Clashscore	1.25	1.3
No. atoms Protein Ligand/Water	 2867 324	 2843 133
B-factors Protein Ligand/ion Water	 20.97 37.94 32.05	 42.57 67.62 45.05
R.m.s. deviations Bond lengths (Å) Bond angles (°)	 0.005 0.88	 0.008 0.91

Supplementary Figure S1

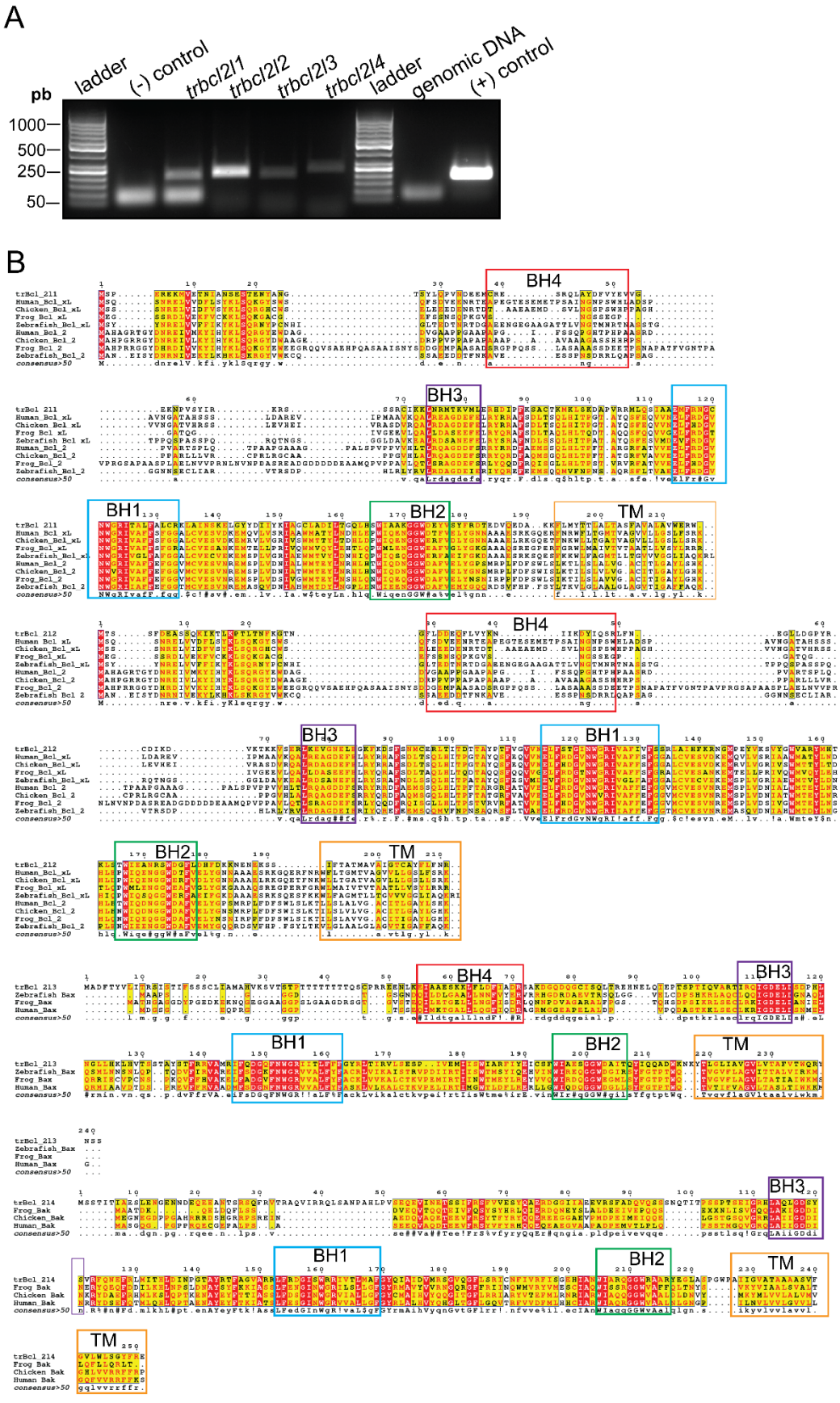

Supplementary Figure S1: Expression and analysis of trBcl-2-like protein primary structures. **(A**) RT-PCR on RNA extracted from whole Trichoplax animals. *TrBcl2like* gene expression was detected using specific exon internal primers. DNA (negative control) as well as genomic DNA were used as negative controls. L1 primers amplifying plasmid DNA encoding *trbcl2l1* ORF was used as a positive PCR control. **(B)** ClustalW alignments of trBcl-2-like proteins with characterized Bcl-2 homologs from multiple species. Sequences corresponding to the BH and TM motifs were highlighted with colored boxes.

Supplementary Figure S2

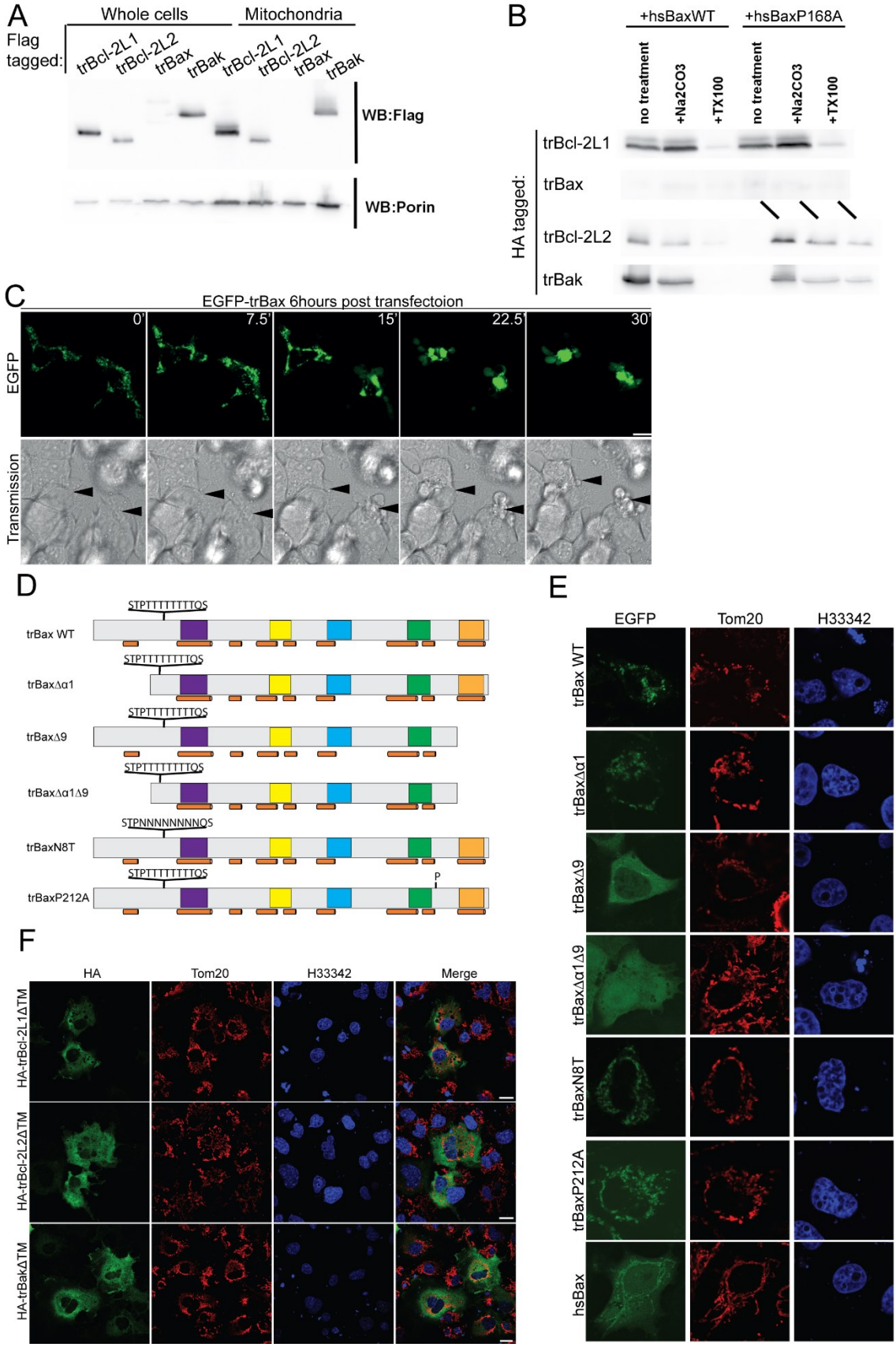

Supplementary Figure S2: Analysis of trBcl-2like protein localization.

(A) Western-blot analysis of trBcl-2like protein expression in yeast mitochondria. Whole cell extracts (from ~200,000 cells) or isolated mitochondria (50µg protein) were loaded onto SDS-PAGE, blotted, and analysed using anti-Flag (mouse monoclonal, Sigma) anti-yeast porin (mouse monoclonal, Thermofisher) antibodies. **(B)** Mitochondria isolated from strains co-expressing WT-Bax or BaxP168A and the different trBcl-2like proteins were suspended (1 mg/ml) in 0.6M mannitol, 2mM EGTA, 10mM tris/maleate, pH 7.0, and supplemented with 0.1 ml of 1M Na_2CO_3 (pH 10.0) or 1% Triton X100, and samples were incubated for 10 minutes on ice. They were centrifuged (10 minutes, 27,000 g), and pellets were analysed by western-blotting for the presence of trBcl-2-like proteins. **(C)** Representative confocal images showing the intracellular localization of EGFPtrBax-expressing BMK DKO cells. TrBax was rapidly translocated to the mitochondria where it led to rapid cell shrinkage and blebbing. Scale bar: 10 µm. **(D)** Schematic representation of the primary structures of WT- trBax and associated mutants. The positions of conserved BH1-BH4 motifs and of the C-terminal transmembrane motif (TM) as well as the locations of the predicted alpha helices are indicated with colored boxes and brown cylinders, respectively. The mucin like site is indicated in the N-terminal region. **(E)** Representative confocal images showing the subcellular localization of EGFP-tagged WT-trBax and associated mutants as well as human (hs) Bax. Mitochondria were labeled using anti-Tom20 antibody. Merged channels between EGFP and Tom20 were presented on the right. Scale bar: 20 µm. **(F)** Representative confocal images showing the subcellular localization of HA-tagged trBcl-2-like ΔTM mutants. Mitochondria were labeled using anti-Tom20 antibody. HA fusion proteins were detected using anti-HA antibody. Merged channels between HA and Tom20 were presented on the right. Scale bar: 20 µm.

Supplementary Figure S3

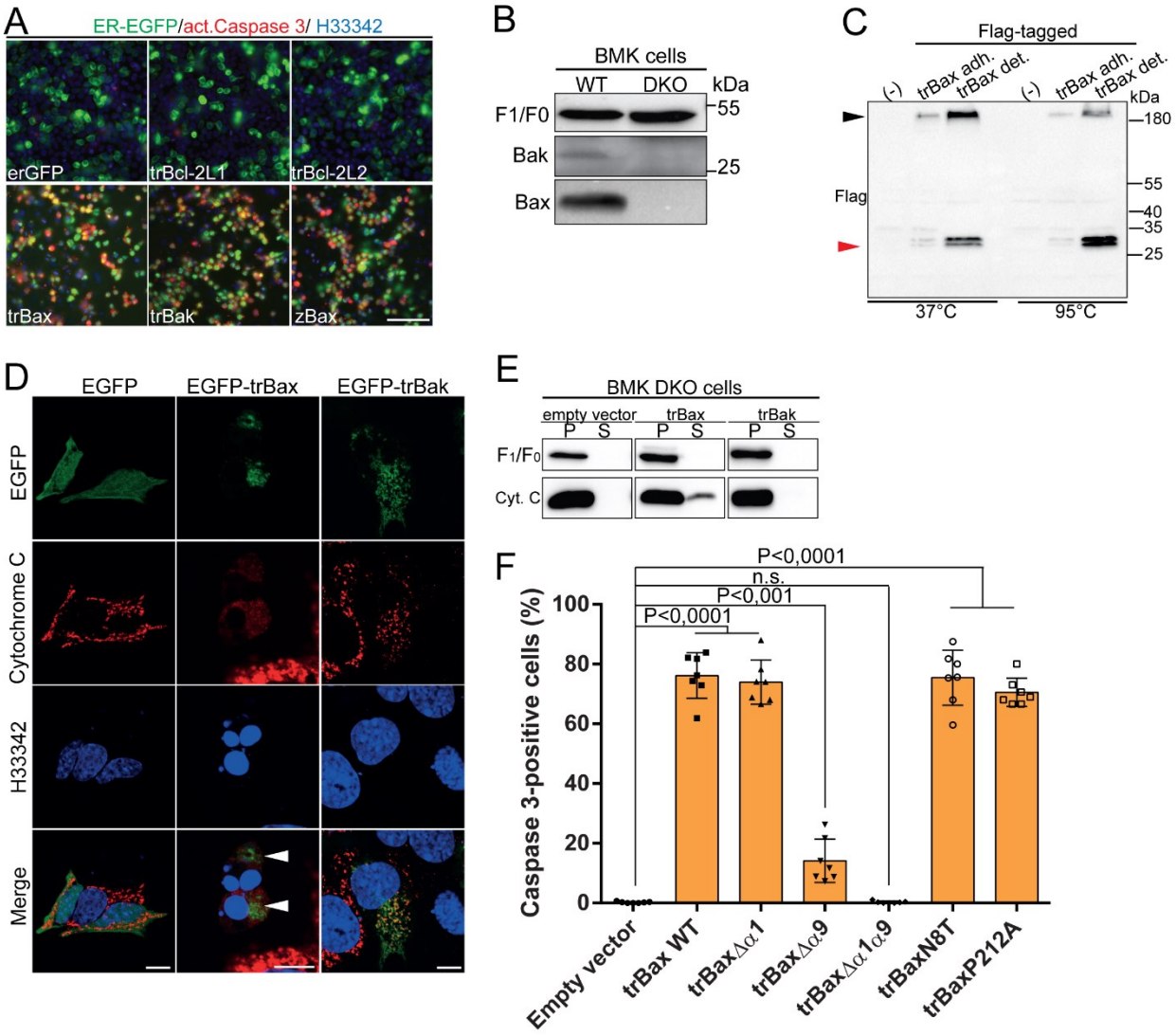

Supplementary Figure S3: Control of MOMP by TrBcl-2-like proteins.

(A) Representative fluorescence microscopy images of the effect of trBcl-2-like protein expression on Caspase 3 activation in HeLa cells. Cells were transfected with ER-EGFP expressing vector alone or in combination with trBcl-2-like proteins and stained with an anti-activated Caspase 3 antibody and counterstained with the nuclear dye H33342. ER-EGFP and the zebrafish ortholog of Bax (zBax) were used as negative and positive controls, respectively. Scale bar: 100 µm. **(B)** Immunoblot showing the content of endogenous Bax and Bak proteins in BMK WT versus BMK *bax -/-, bak-/-* double knock-out cells. F_1F_0 ATPase was used as a loading control. **(C)** Western blot (100 µg total proteins) of protein extracts obtained from detached cells (det) and adherent cells (adh) expressing Flag-tagged trBax or transfected with empty vector (-). TrBax was highly enriched in the detached cells where it was detected as a multiprotein complex (black arrowhead) resistant to Laemmli treatment at 37°C, but became monomeric (red arrowhead) once the temperature was raised to 95°C for 5 min. **(D)** Representative confocal images showing the subcellular distribution

of cytochrome c in EGFP-, EGFP-trBax- and EGFP-trBak-expressing BMK DKO cells. In control EGFP-trBak cells, cytochrome c has a mitochondrial localization and becomes cytosolic following trBax induced MOMP. Scale bar: 20 μm **(E)** Immunoblot showing the results of cytochrome c release assay performed in BMK DKO cells. Cells transfected with empty vector or vector expressing trBax or trBak were subjected to Digitonin treatment (25 μg/mL) for 5 min. Cells were then separated by centrifugation into a pellet (P) fraction containing mitochondrial membranes, and a supernatant (S) containing soluble proteins. The two fractions were immunostained with anti-cytochrome c and anti-F_1F_0 ATPase antibodies. **(F)** Histogram showing the effect of expression of WT-trBax and associated mutants on Caspase 3 activation in BMK DKO cells. Deletion of the TM motif significantly impairs the pro-apoptotic activity of trBax (mean ± SD; three independent experiments, one-way ANOVA statistical analysis, n.s.: not significant).

Supplementary Figure S4

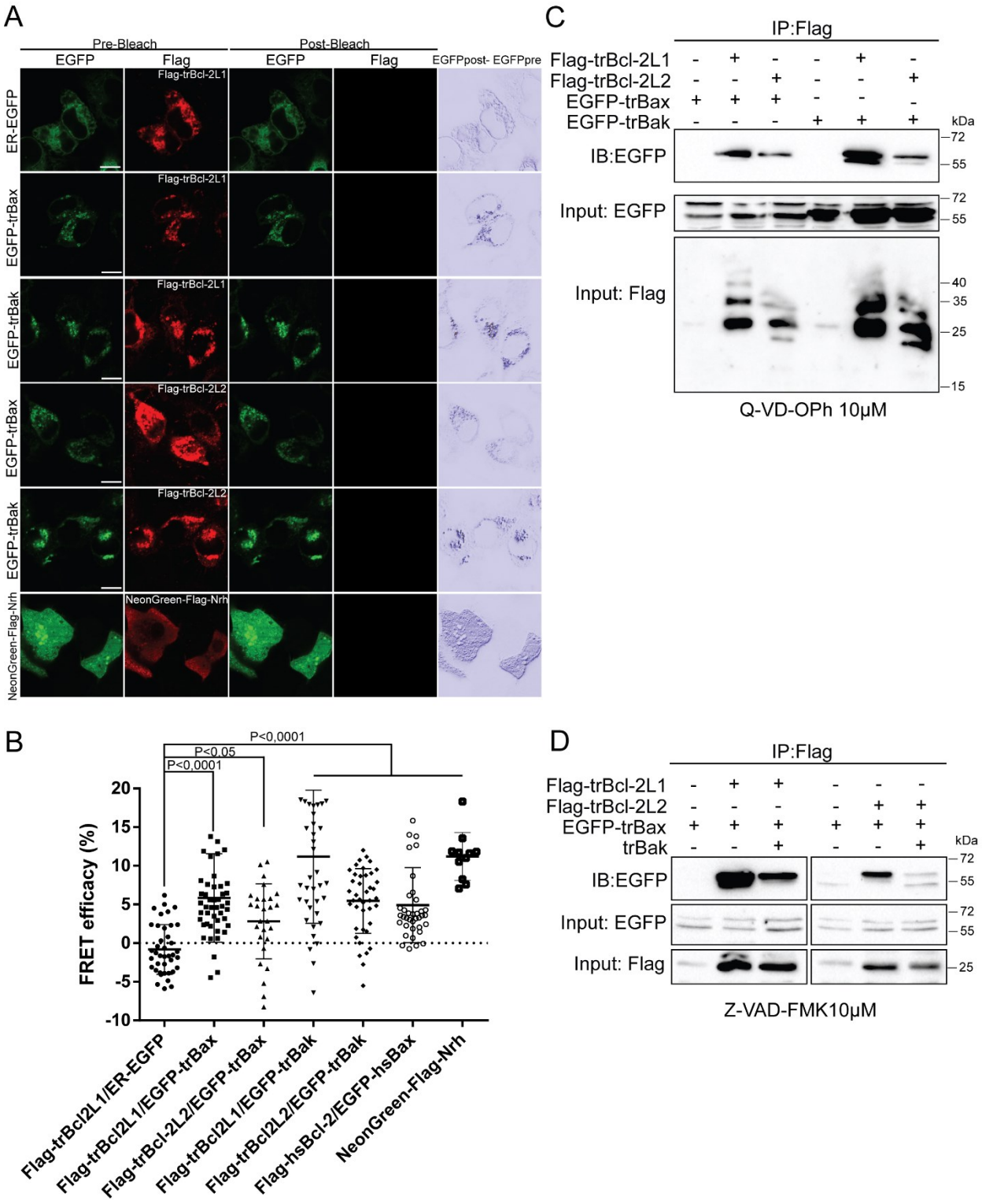

Supplementary Figure S4: FRET-based interaction assay of trBcl-2 proteins.

(A) Representative confocal images demonstrating the changes in EGFP (donor) fluorescence following Alexafluor 568 (acceptor) photobleaching. BMK cells expressing different combinations of EGFP-tagged trBax and Bak and Flag tagged trBcl-2L1 and trBcl-2L2 were fixed and immunostained with anti-Flag primary and anti-mouse IgG secondary antibodies linked with the

Alexa568 fluorophore. Subtractions of EGFP fluorescence before and after photobleaching are shown in the right-hand column. NeonGreen-Flag-Nrh protein was used as positive control. Scale bar: 10 µm. **(B)** Scatter plot graph showing the results from FRET-based interaction analyses between an EGFP donor and an Alexa568 acceptor. Interactions between trBcl-2-like proteins were estimated by measuring the dequenching of EGFP emission induced by Alexa568 photobleaching (mean ± SD; three independent experiments, one-way ANOVA statistical analysis). **(C)** Immunoblot analysis of co-immunoprecipitation between Flag-tagged trBcl-2L1, trBcl-2L2 and EGFP-tagged trBax and trBak proteins. TrBcl-2L1 and –L2 proteins interact with trBax and trBak. Q-VD-OPh (10 µM) was used to prevent caspase activation and subsequent cell detachment. **(D)** Immunoblot analysis of co-immunoprecipitation between Flag-tagged trBcl-2L1, trBcl-2L2 and EGFP-tagged trBax in absence or presence of trBak protein. The co-expression of trBak decreases the binding of trBax to the anti-apoptotic trBcl-2L1 and –L2 proteins. Z-VAD-FMK (10 µM) was used to prevent caspase activation and subsequent cell detachment.

Supplementary Figure S5

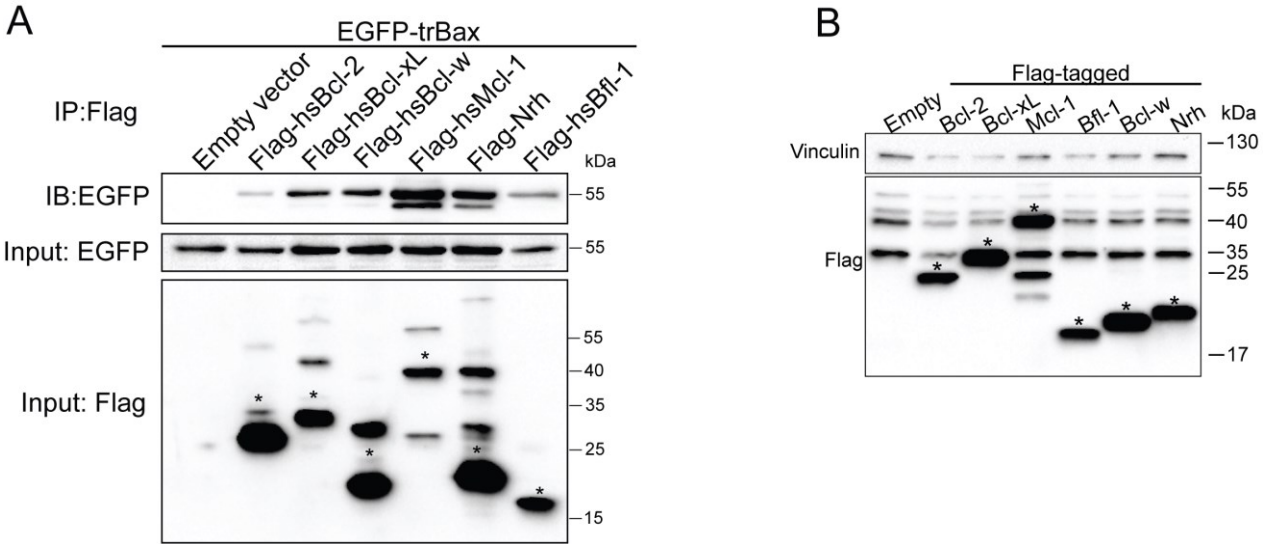

Supplementary Figure S5: Expression and interaction of human Bcl-2 homologs with trBax. **(A)** Immunoblot analysis of co-immunoprecipitation between Flag-tagged human Bcl-2 homologs and EGFP-tagged full-length trBax protein. TrBax binds more efficiently to hsMcl-1 compared to hsBcl-2 or hsBcl-x_L. Asterisks denote the bands corresponding to the predicted molecular weights of human Bcl-2 proteins. **(B)** Immunoblot analysis of the expression of Flag-tagged human Bcl-2 homologs in BMK DKO cells. Vinculin was used as loading control. Asterisks denote the bands corresponding to the predicted molecular weights of human Bcl-2 proteins.

Supplementary Figure S6

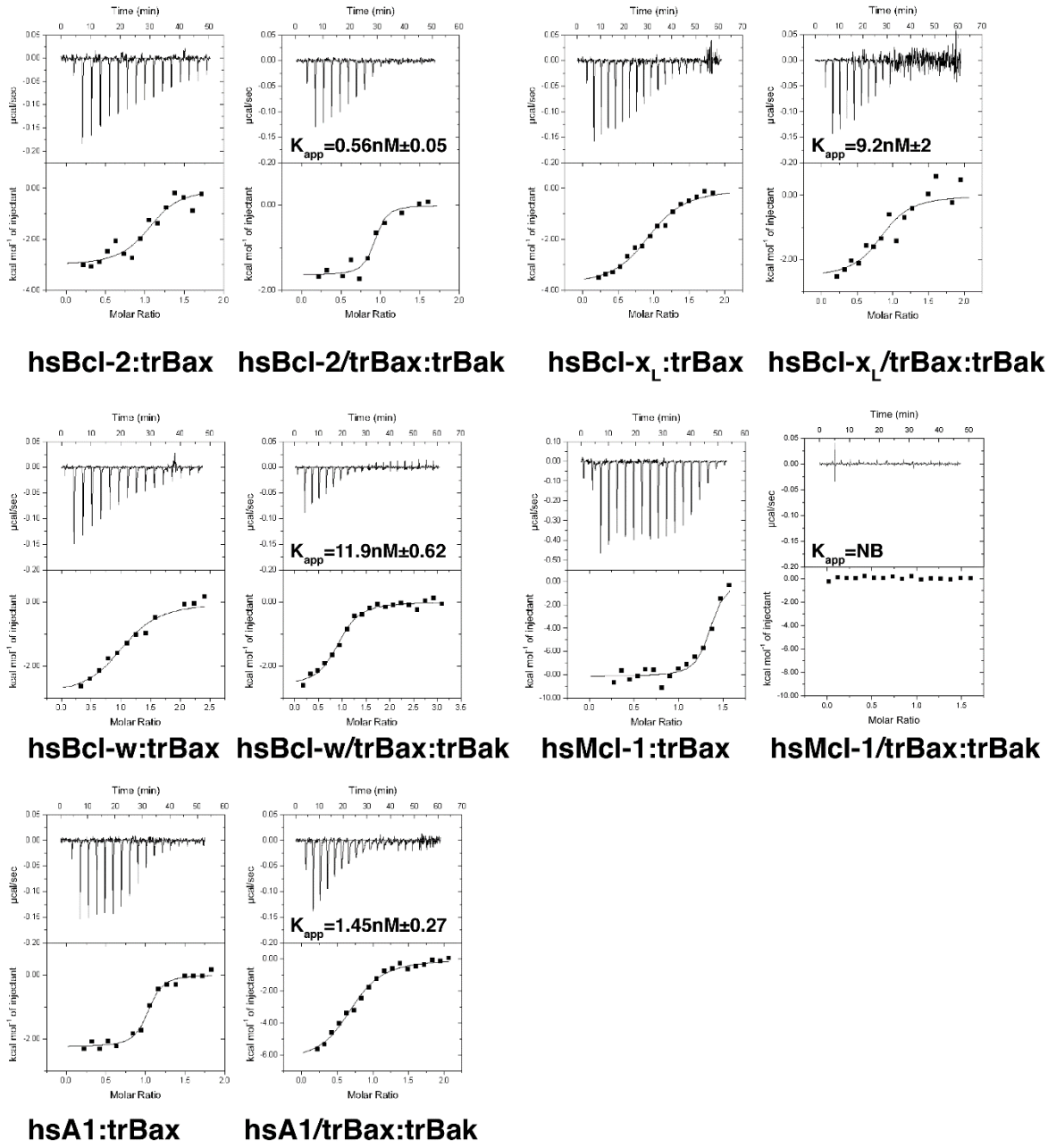

Supplementary Figure S6: Competition isothermal titration calorimetry of trBax BH3 and trBak BH3 with human anti-apoptotic Bcl-2 proteins.

Human anti-apoptotic Bcl-2 proteins bound to peptides spanning the trBax BH3 motif are titrated with trBak BH3 peptide. Human anti-apoptotic Bcl-2 proteins are titrated with trBax BH3 prior to a second titration of the saturated human Bcl-2:trBax BH3 complex with trBak BH3. Apparent affinity constants were determined by ITC using a competitive binding model, and apparent affinity or K_{APP} values (in nM) are the means of 3 experiments ± SD. NB: not bound.

Supplementary Materials and Methods

Co-immunoprecipitation

Immunoprecipitation experiments were performed on HeLa cells. Cells at 80-90% confluence in 10 cm plates were transfected with 2,5 µg pEGFP-C1-trBax or pEGFP-C1-hsBax in combination with pCS2+ empty vector (7,5µg), pCS2+Flag-trBcl-2L1 (5µg), -L2 (5µg), hsBcl-2 (5µg), hsBcl-xL(5µg), hsBcl-w (5µg), hsMcl-1 or Nrh, hsBfl-1. The total quantity of transfected DNA per condition was 10µg and was ensured by adding the required quantity of pCS2+ empty vector. DNA transfection was performed using X-tremeGENE™ HP DNA Transfection Reagent (Roche) according to the manufacturer's protocol. Twenty-four hours later, cells were lysed in TNE buffer (10 mM Tris-HCl, 200 mM NaCl, 1 mM EDTA [pH 7.4], 0,2% NP-40, containing protease inhibitors). Extracts were incubated overnight at 4°C with 20 µL of Anti Flag M2 magnetic beads (Sigma Aldrich). Pellets containing immunoprecipitated fractions were washed three times in TNE buffer and analyzed by immunoblotting.

Zebrafish experiments

Zebrafish (crosses between AB and TU strains) were raised and maintained at 28.5°C according to standard procedures (*54*). Embryos were collected after fertilization and injected at the one-cell stage with *in vitro* transcribed mRNA encoding trBcl-2L1 to -2L4 proteins (100 pg total mRNA/ embryo) using mMESSAGE mMACHINE SP6 Transcription Kit (Thermo Fischer). Embryo death was monitored at regular intervals for 6 h post-fertilization.

Yeast experiments

The four Trichoplax cDNAs encoding proteins harboring a Flag tag at their N-termini end were cloned using the BamHI/XhoI sites of the pYES2 plasmid downstream of the inducible promoter GAL1/10.

The diploid yeast strain W303 (mat a/mat α, ade1/ade1, his3/his3, leu2/leu2, trp1/trp1, ura3/ura3) was used in all experiments. Cells were co-transformed with pYES2-TrBcl-2-like plasmids and pYES3-Bax plasmids. Two Bax variants were used: BaxWT coding the full-length untagged human protein, and BaxP168A carrying the P168A substitution that converts Bax into a constitutively membrane-inserted and active protein (*30, 55*).

Transformants were selected on YNB plates supplemented with glucose and without uracil and tryptophan. For Bax and trBcl-2like protein expression, cells were grown aerobically at 28°C in YNB liquid medium (Yeast Nitrogen Base, 0.17%, potassium phosphate 0.1%, ammonium

sulfate 0.5%, Drop-Mix 0.2%, auxotrophic requirements 0.01%) supplemented with 2% DL-lactate as a carbon source. After reaching a cell density of 10^6 cells/mL, 0.8% galactose was added to induce the expression of Bax and trBcl-2-like proteins. The expression was induced overnight (16 hours). Mitochondria isolation, western-blot analyses on whole cell extracts and isolated mitochondria were performed as described previously (*56*).

Supplementary Table S2: Sequence of oligonucleotide primers used for this study

Vectors/ Purpose	Constructs	Primers
pJET1.2/blunt cDNA cloning & Sequencing	trBcl-2L1	5'ATGTCTCCTGAACGCGAAAAAATGG
		5'TCACCATCTTTCCCACACTGCAAGCG
	trBcl-2L2	5'ATGACATCTTCCTTCGATGAGGCATC
		5'TTATCTATTAAACAGAAAGTATGCACAAGTACC
	trBcl-2L3 (trBax)	5'ATGGCCGATTTCACGTATGTACTGA
		5'TTAGCTACTGTTATATCGTTGCCATGTG
	trBcl-2L4 (trBak)	5'ATGTCTAGCACTATTACAATAGCTGAATCGC
		5'TTATTCTCTAAAATAGCCTGAAAGCCATAGG
PCR products Exon1/ Gene expression	trBcl-2L1	5'TCCGTAATGGCTGCAACTGG
		5'CTCACGTACTCATCCCAGCC
	trBcl-2L2	5'GCTTACCCAACGTTTGTGGG
		5'TGTTCGCTTCGATCCAGGTAG
	trBcl-2L3 (trBax)	5'CCACCACTACTCAGTCATGTCC
		5'TGTTGGTGACGTCGGTTCAA
	trBcl-2L4 (trBak)	5'CTATCGGCAAATCCGGCTCA
		5'TGCGCTAAATGGCGTCCTAT
pCS2+/ Subcellular localization	HA-trBcl-2L1ΔTM	5'ATATGGATCCATGTACCCATACGATGTTCCAGATTACGCTATGTCTC CTGAACGCGAAAAAATGG
		5'ATATCTCGAGTCATTTTTTTGCATCTTCTTGTAC
	HA-trBcl-2L2ΔTM	5'ATATGGATCCATGTACCCATACGATGTTCCAGATTACGCTATGACAT CTTCCTTCGATGAGGCATC
		5'ATATCTCGAGTCAAGACTTTTCATTCTCATTTTTC
	HA-trBakΔTM	5'ATATGGATCCATGTACCCATACGATGTTCCAGATTACGCTATGTCTA GCACTATTACAATAGC
		5'ATATCTCGAGTCACCCAGGCGAAGCAAGTCCTTCGTA
	3xFlag-trBax	5'ATATGAATTCGCCGATTTCACGTATGTACTGA
		5'ATATCTCGAGTTAGCTACTGTTATATCG
PEGFP-C1/subcellular localization & cell death assay	EGFP-trBax-opt-WT	5'ATATAGATCTATGGCTGACTTCACATATGTG
		5'ATATGAATTCCTAGCTGCTGTTGTAGCGCTGC
	EGFP-trBax-opt-Δα1	5' GTGTAGATCTAAGTCCGTGACTTCCACACCAACGA
		5'ATATGAATTCCTAGCTGCTGTTGTAGCGCTGC
	EGFP-trBax-opt-Δ9	5'ATATAGATCTATGGCTGACTTCACATATGTG
		5'ATATGAATTCCTAGCTGCTGTTGTAGCGCTGC
	EGFP-trBax-opt-Δ1Δ9	5'GTGTAGATCTAAGTCCGTGACTTCCACACCAACGA
		5'ATATGAATTCCTAGCTGCTGTTGTAGCGCTGC
	EGFP-trBax-opt-P212A	5'TATATACAGCAACCGGACTGGAAGAACAAAT
		5'ATTTGTTCTTCCAGTCCGGTTGCTGTATATA
	EGFP-trBax BH3	5'ATATAGATCTATCGAGCCAACGTCACCAAC
		5'ATATGAATTCTCAATTGAGATGGGGATCGCTGTC
	EGFP-trBak BH3	5'ATATAGATCTCCATCATCTCCTACATCTGAAA
		5'ATATGAATTCTCATTCATTTTGGAAACGGACACTA

REFERENCES AND NOTES

1. C. M. Zmasek, A. Godzik, Evolution of the animal apoptosis network. *Cold Spring Harb. Perspect. Biol.* **5**, a008649 (2013).
2. Y. Fuchs, H. Steller, Live to die another way: Modes of programmed cell death and the signals emanating from dying cells. *Nat. Rev. Mol. Cell Biol.* **16**, 329–344 (2015).
3. S. Banjara, C. D. Suraweera, M. G. Hinds, M. Kvansakul, The Bcl-2 family: Ancient origins, conserved structures, and divergent mechanisms. *Biomolecules* **10**, 128 (2020).
4. M. O. Hengartner, R. E. Ellis, H. R. Horvitz, *Caenorhabditis elegans* gene *ced-9* protects cells from programmed cell death. *Nature* **356**, 494–499 (1992).
5. L. Quinn, M. Coombe, K. Mills, T. Daish, P. Colussi, S. Kumar, H. Richardson, Buffy, a *Drosophila* Bcl-2 protein, has anti-apoptotic and cell cycle inhibitory functions. *EMBO J.* **22**, 3568–3579 (2003).
6. M. Lasi, B. Pauly, N. Schmidt, M. Cikala, B. Stiening, T. Käsbauer, G. Zenner, T. Popp, A. Wagner, R. T. Knapp, A. H. Huber, M. Grunert, J. Söding, C. N. David, A. Böttger, The molecular cell death machinery in the simple cnidarian *Hydra* includes an expanded caspase family and pro- and anti-apoptotic Bcl-2 proteins. *Cell Res.* **20**, 812–825 (2010).
7. E. Kratz, P. M. Eimon, K. Mukhyala, H. Stern, J. Zha, A. Strasser, R. Hart, A. Ashkenazi, Functional characterization of the *Bcl-2* gene family in the zebrafish. *Cell Death Differ.* **13**, 1631–1640 (2006).
8. E. F. Lee, O. B. Clarke, M. Evangelista, Z. Feng, T. P. Speed, E. B. Tchoubrieva, A. Strasser, B. H. Kalinna, P. M. Colman, W. D. Fairlie, Discovery and molecular characterization of a Bcl-2-regulated cell death pathway in schistosomes. *Proc. Natl. Acad. Sci. U.S.A.* **108**, 6999–7003 (2011).
9. R. Singh, A. Letai, K. Sarosiek, Regulation of apoptosis in health and disease: The balancing act of BCL-2 family proteins. *Nat. Rev. Mol. Cell Biol.* **20**, 175–193 (2019).
10. M. Kvansakul, M. G. Hinds, The structural biology of BH3-only proteins. *Methods Enzymol.* **544**, 49–74 (2014).
11. A. Strasser, D. L. Vaux, Viewing BCL2 and cell death control from an evolutionary perspective. *Cell Death Differ.* **25**, 13–20 (2018).
12. J. Kale, E. J. Osterlund, D. W. Andrews, BCL-2 family proteins: Changing partners in the dance towards death. *Cell Death Differ.* **25**, 65–80 (2018).

13. S. W. G. Tait, A. Oberst, G. Quarato, S. Milasta, M. Haller, R. Wang, M. Karvela, G. Ichim, N. Yatim, M. L. Albert, G. Kidd, R. Wakefield, S. Frase, S. Krautwald, A. Linkermann, D. R. Green, Widespread mitochondrial depletion via mitophagy does not compromise necroptosis. *Cell Rep.* **5**, 878–885 (2013).
14. T. Moldoveanu, A. V. Follis, R. W. Kriwacki, D. R. Green, Many players in BCL-2 family affairs. *Trends Biochem. Sci.* **39**, 101–111 (2014).
15. S. Caria, M. G. Hinds, M. Kvansakul, Structural insight into an evolutionarily ancient programmed cell death regulator – the crystal structure of marine sponge BHP2 bound to LB-Bak-2. *Cell Death Dis.* **8**, e2543 (2017).
16. C. Galasso, S. D'Aniello, C. Sansone, A. Ianora, G. Romano, Identification of cell death genes in sea urchin *Paracentrotus lividus* and their expression patterns during embryonic development. *Genome Biol. Evol.* **11**, 586–596 (2019).
17. A. Moya, K. Sakamaki, B. M. Mason, L. Huisman, S. Forêt, Y. Weiss, T. E. Bull, K. Tomii, K. Imai, D. C. Hayward, E. E. Ball, D. J. Miller, Functional conservation of the apoptotic machinery from coral to man: The diverse and complex Bcl-2 and caspase repertoires of *Acropora millepora*. *BMC Genomics* **17**, 62 (2016).
18. K. L. O'Neill, K. Huang, J. Zhang, Y. Chen, X. Luo, Inactivation of prosurvival Bcl-2 proteins activates Bax/Bak through the outer mitochondrial membrane. *Genes Dev.* **30**, 973 (2016).
19. K. Huang, K. L. O'Neill, J. Li, W. Zhou, N. Han, X. Pang, W. Wu, L. Struble, G. Borgstahl, Z. Liu, L. Zhang, X. Luo, BH3-only proteins target BCL-xL/MCL-1, not BAX/BAK, to initiate apoptosis. *Cell Res.* **29**, 942–952 (2019).
20. D. Shu, Y. Isozaki, X. Zhang, J. Han, S. Maruyama, Birth and early evolution of metazoans. *Gondwana Res.* **25**, 884–895 (2014).
21. H.-J. Osigus, S. Rolfes, R. Herzog, K. Kamm, B. Schierwater, *Polyplacotoma mediterranea* is a new ramified placozoan species. *Curr. Biol.* **29**, R148–R149 (2019).
22. T. Syed, B. Schierwater, *Trichoplax adhaerens*: Discovered as a missing link, forgotten as a hydrozoan, re-discovered as a key to metazoan evolution. *Vie Milieu* **52**, 177–187 (2002).
23. B. Schierwater, My favorite animal, *Trichoplax adhaerens*. *BioEssays* **27**, 1294–1302 (2005).
24. M. Srivastava, E. Begovic, J. Chapman, N. H. Putnam, U. Hellsten, T. Kawashima, A. Kuo, T. Mitros, A. Salamov, M. L. Carpenter, A. Y. Signorovitch, M. A. Moreno, K. Kamm, J.

Grimwood, J. Schmutz, H. Shapiro, I. V. Grigoriev, L. W. Buss, B. Schierwater, S. L. Dellaporta, D. S. Rokhsar, The *Trichoplax* genome and the nature of placozoans. *Nature* **454**, 955–960 (2008).

25. D. R. Green, P. Fitzgerald, Just so stories about the evolution of apoptosis. *Curr. Biol.* **26**, R620–R627 (2016).
26. N. Popgeorgiev, L. Jabbour, G. Gillet, Subcellular localization and dynamics of the Bcl-2 family of proteins. *Front. Cell. Dev. Biol.* **6**, 13 (2018).
27. P.-F. Cartron, H. Arokium, L. Oliver, K. Meflah, S. Manon, F. M. Vallette, Distinct domains control the addressing and the insertion of Bax into mitochondria. *J. Biol. Chem.* **280**, 10587–10598 (2005).
28. F. Edlich, S. Banerjee, M. Suzuki, M. M. Cleland, D. Arnoult, C. Wang, A. Neutzner, N. Tjandra, R. J. Youle, Bcl-x_L retrotranslocates Bax from the mitochondria into the cytosol. *Cell* **145**, 104–116 (2011).
29. A. Schinzel, T. Kaufmann, M. Schuler, J. Martinalbo, D. Grubb, C. Borner, Conformational control of Bax localization and apoptotic activity by Pro168. *J. Cell Biol.* **164**, 1021–1032 (2004).
30. L. Simonyan, A. Légiot, I. Lascu, G. Durand, M.-F. Giraud, C. Gonzalez, S. Manon, The substitution of Proline 168 favors Bax oligomerization and stimulates its interaction with LUVs and mitochondria. *Biochim. Biophys. Acta Biomembr.* **1859**, 1144–1155 (2017).
31. N. Popgeorgiev, B. Bonneau, K. F. Ferri, J. Prudent, J. Thibaut, G. Gillet, The apoptotic regulator Nrz controls cytoskeletal dynamics via the regulation of Ca^{2+} trafficking in the zebrafish blastula. *Dev. Cell* **20**, 663–676 (2011).
32. A. Aouacheria, F. Brunet, M. Gouy, Phylogenomics of life-or-death switches in multicellular animals: Bcl-2, BH3-Only, and BNip families of apoptotic regulators. *Mol. Biol. Evol.* **22**, 2395–2416 (2005).
33. A. Aouacheria, V. Rech de Laval, C. Combet, J. M. Hardwick, Evolution of Bcl-2 homology motifs: Homology versus homoplasy. *Trends Cell Biol.* **23**, 103–111 (2013).
34. J. J. Chou, H. Li, G. S. Salvesen, J. Yuan, G. Wagner, Solution structure of BID, an intracellular amplifier of apoptotic signaling. *Cell* **96**, 615–624 (1999).

35. J. M. McDonnell, D. Fushman, C. L. Milliman, S. J. Korsmeyer, D. Cowburn, Solution structure of the proapoptotic molecule BID: A structural basis for apoptotic agonists and antagonists. *Cell* **96**, 625–634 (1999).
36. R. Thijssen, A. W. Roberts, Venetoclax in lymphoid malignancies: New insights, more to learn. *Cancer Cell* **36**, 341–343 (2019).
37. R. Beroukhim, C. H. Mermel, D. Porter, G. Wei, S. Raychaudhuri, J. Donovan, J. Barretina, J. S. Boehm, J. Dobson, M. Urashima, K. T. McHenry, R. M. Pinchback, A. H. Ligon, Y.-J. Cho, L. Haery, H. Greulich, M. Reich, W. Winckler, M. S. Lawrence, B. A. Weir, K. E. Tanaka, D. Y. Chiang, A. J. Bass, A. Loo, C. Hoffman, J. Prensner, T. Liefeld, Q. Gao, D. Yecies, S. Signoretti, E. Maher, F. J. Kaye, H. Sasaki, J. E. Tepper, J. A. Fletcher, J. Tabernero, J. Baselga, M.-S. Tsao, F. Demichelis, M. A. Rubin, P. A. Janne, M. J. Daly, C. Nucera, R. L. Levine, B. L. Ebert, S. Gabriel, A. K. Rustgi, C. R. Antonescu, M. Ladanyi, A. Letai, L. A. Garraway, M. Loda, D. G. Beer, L. D. True, A. Okamoto, S. L. Pomeroy, S. Singer, T. R. Golub, E. S. Lander, G. Getz, W. R. Sellers, M. Meyerson, The landscape of somatic copy-number alteration across human cancers. *Nature* **463**, 899–905 (2010).
38. K. J. Campbell, S. Dhayade, N. Ferrari, A. H. Sims, E. Johnson, S. M. Mason, A. Dickson, K. M. Ryan, G. Kalna, J. Edwards, S. W. G. Tait, K. Blyth, MCL-1 is a prognostic indicator and drug target in breast cancer. *Cell Death Dis.* **9**, 19 (2018).
39. Z. Xiang, H. Luo, J. E. Payton, J. Cain, T. J. Ley, J. T. Opferman, M. H. Tomasson, Mcl1 haploinsufficiency protects mice from Myc-induced acute myeloid leukemia. *J. Clin. Invest.* **120**, 2109–2118 (2010).
40. I. K. Zervantonakis, C. Iavarone, H.-Y. Chen, L. M. Selfors, S. Palakurthi, J. F. Liu, R. Drapkin, U. Matulonis, J. D. Leverson, D. Sampath, G. B. Mills, J. S. Brugge, Systems analysis of apoptotic priming in ovarian cancer identifies vulnerabilities and predictors of drug response. *Nat. Commun.* **8**, 365 (2017).
41. A. Kotschy, Z. Szlavik, J. Murray, J. Davidson, A. L. Maragno, G. Le Toumelin-Braizat, M. Chanrion, G. L. Kelly, J.-N. Gong, D. M. Moujalled, A. Bruno, M. Csekei, A. Paczal, Z. B. Szabo, S. Sipos, G. Radics, A. Proszenyak, B. Balint, L. Ondi, G. Blasko, A. Robertson, A. Surgenor, P. Dokurno, I. Chen, N. Matassova, J. Smith, C. Pedder, C. Graham, A. Studeny, G. Lysiak-Auvity, A.-M. Girard, F. Gravé, D. Segal, C. D. Riffkin, G. Pomilio, L. C. A. Galbraith, B. J. Aubrey, M. S. Brennan, M. J. Herold, C. Chang, G. Guasconi, N. Cauquil, F.

Melchiore, N. Guigal-Stephan, B. Lockhart, F. Colland, J. A. Hickman, A. W. Roberts, D. C. S. Huang, A. H. Wei, A. Strasser, G. Lessene, O. Geneste, The MCL1 inhibitor S63845 is tolerable and effective in diverse cancer models. *Nature* **538**, 477–482 (2016).

42. M. Eitel, B. Schierwater, The phylogeography of the Placozoa suggests a taxon-rich phylum in tropical and subtropical waters. *Mol. Ecol.* **19**, 2315–2327 (2010).
43. E. Arnaud, K. F. Ferri, J. Thibaut, Z. Haftek-Terreau, A. Aouacheria, D. Le Guellec, T. Lorca, G. Gillet, The zebrafish bcl-2 homologue Nrz controls development during somitogenesis and gastrulation via apoptosis-dependent and -independent mechanisms. *Cell Death Differ.* **13**, 1128–1137 (2006).
44. Y.-P. Rong, A. S. Aromolaran, G. Bultynck, F. Zhong, X. Li, K. M. Coll, S. Matsuyama, S. Herlitze, H. L. Roderick, M. D. Bootman, G. A. Mignery, J. B. Parys, H. De Smedt, C. W. Distelhorst, Targeting Bcl-2-IP3 receptor interaction to reverse Bcl-2's inhibition of apoptotic calcium signals. *Mol. Cell* **31**, 255–265 (2008).
45. F. W. Studier, Protein production by auto-induction in high density shaking cultures. *Protein Expr. Purif.* **41**, 207–234 (2005).
46. B. Marshall, H. Puthalakath, S. Caria, S. Chugh, M. Doerflinger, P. M. Colman, M. Kvansakul, Variola virus F1L is a Bcl-2-like protein that unlike its vaccinia virus counterpart inhibits apoptosis independent of Bim. *Cell Death Dis.* **6**, e1680 (2015).
47. W. Kabsch, Integration, scaling, space-group assignment and post-refinement. *Acta Crystallogr. D Biol. Crystallogr.* **66**, 133 (2010).
48. A. J. McCoy, Solving structures of protein complexes by molecular replacement with Phaser. *Acta Crystallogr. D Biol. Crystallogr.* **63**, 32–41 (2007).
49. X. Liu, S. Dai, Y. Zhu, P. Marrack, J. W. Kappler, The structure of a Bcl-x_L/Bim fragment complex: Implications for Bim function. *Immunity* **19**, 341–352 (2003).
50. P. Emsley, B. Lohkamp, W. G. Scott, K. Cowtan, Features and development of Coot. *Acta Crystallogr. D. Biol. Crystallogr.* **66**, 486–501 (2010).
51. N. Echols, R. W. Grosse-Kunstleve, P. V. Afonine, G. Bunkóczi, V. B. Chen, J. J. Headd, A. J. McCoy, N. W. Moriarty, R. J. Read, D. C. Richardson, J. S. Richardson, T. C. Terwilliger, P. D. Adams, Graphical tools for macromolecular crystallography in PHENIX. *J. Appl. Crystallogr.* **45**, 581–586 (2012).

52. A. Morin, B. Eisenbraun, J. Key, P. C. Sanschagrin, M. A. Timony, M. Ottaviano, P. Sliz, Collaboration gets the most out of software. *eLife* **2**, e01456 (2013).
53. P. A. Meyer, S. Socias, J. Key, E. Ransey, E. C. Tjon, A. Buschiazzo, M. Lei, C. Botka, J. Withrow, D. Neau, K. Rajashankar, K. S. Anderson, R. H. Baxter, S. C. Blacklow, T. J. Boggon, A. M. J. J. Bonvin, D. Borek, T. J. Brett, A. Caflisch, C.-I. Chang, W. J. Chazin, K. D. Corbett, M. S. Cosgrove, S. Crosson, S. Dhe-Paganon, E. D. Cera, C. L. Drennan, M. J. Eck, B. F. Eichman, Q. R. Fan, A. R. Ferré-D'Amaré, J. C. Fromme, K. C. Garcia, R. Gaudet, P. Gong, S. C. Harrison, E. E. Heldwein, Z. Jia, R. J. Keenan, A. C. Kruse, M. Kvansakul, J. S. McLellan, Y. Modis, Y. Nam, Z. Otwinowski, E. F. Pai, P. J. B. Pereira, C. Petosa, C. S. Raman, T. A. Rapoport, A. Roll-Mecak, M. K. Rosen, G. Rudenko, J. Schlessinger, T. U. Schwartz, Y. Shamoo, H. Sondermann, Y. J. Tao, N. H. Tolia, O. V. Tsodikov, K. D. Westover, H. Wu, I. Foster, J. S. Fraser, F. R. N. C. Maia, T. Gonen, T. Kirchhausen, K. Diederichs, M. Crosas, P. Sliz, Data publication with the structural biology data grid supports live analysis. *Nat. Commun.* **7**, 10882 (2016).
54. M. Westerfield, *A Guide for the Laboratory Use of Zebrafish Danio (Brachydanio) Rerio* (University of Oregon Press, ed. 3, 1995).
55. H. Arokium, N. Camougrand, F. M. Vallette, S. Manon, Studies of the interaction of substituted mutants of BAX with yeast mitochondria reveal that the C-terminal hydrophobic α-helix is a second ART sequence and plays a role in the interaction with anti-apoptotic BCL-xL. *J. Biol. Chem.* **279**, 52566 (2004).
56. T. T. Renault, O. Teijido, F. Missire, Y. T. Ganesan, G. Velours, H. Arokium, F. Beaumatin, R. Llanos, A. Athané, N. Camougrand, M. Priault, B. Antonsson, L. M. Dejean, S. Manon, Bcl-xL stimulates Bax relocation to mitochondria and primes cells to ABT-737. *Int. J. Biochem. Cell Biol.* **64**, 136 (2015).